Journal of Magnetic Resonance **147,** 266–272 (2000)
doi:10.1006/jmre.2000.2211, available online at http://www.idealibrary.com on IDEAL®

Modified GOESY in the Analysis of Disaccharide Conformation

Ann M. Dixon,* Göran Widmalm,† and T. E. Bull*,[1]

**Laboratory of Biophysics, Office of Vaccines Research and Review, Center for Biologics Evaluation and Research, Food and Drug Administration, Bethesda, Maryland 20893; and †Department of Organic Chemistry, Arrhenius Laboratory, Stockholm University, Stockholm S-106 91, Sweden*

Received May 1, 2000

One-dimensional nuclear magnetic resonance techniques were applied to the conformational investigation of a disaccharide. More specifically, nuclear Overhauser enhancements (NOEs) of protons on either side of the glycosidic bond have been used to determine the conformation of the disaccharide α-L-Rha*p*-(1 $\rightarrow$ 2)-α-L-Rha*p*-OMe. A modified GOESY sequence, incorporating selective excitation and pulsed field gradient enhancement, was developed and used to accurately measure small NOE signals of interest. These experiments were named M-GOESY, for modified GOESY, and the data they provided were used to calculate internuclear distances in the disaccharide molecule. The accuracy of the M-GOESY measurements was enhanced by elimination of indirect effects, or spin diffusion, by selective inversion(s) of either the intermediate magnetization or the source and target magnetization during the mixing time. Results of this study indicate that the α-L-Rha*p*-(1 $\rightarrow$ 2)-α-L-Rha*p*-OMe disaccharide molecule exists primarily in one conformation, with the glycosidic torsion angle $\psi \approx -30°$ based on past molecular dynamics simulations. © 2000 Academic Press

Key Words: **NMR; disaccharide; conformation; 1-D NOE; spin-diffusion.**

INTRODUCTION

Monosaccharides are building blocks of larger oligosaccharide components of glycoproteins and glycolipids. Steric interactions with oligosaccharide components can alter the polarity and solubility of glycoproteins, thus influencing the sequence of folding events and the final tertiary structure. These oligosaccharide components are rich in structural information and present a unique face for both enzyme and receptor recognition of the glycoprotein. Glycolipids also contain oligosaccharides and are found on cell surfaces. Lipopolysaccharides are major components of the outer membranes of Gram-negative bacteria and are the prime targets of antibodies produced by the immune system in response to bacterial infection. Lipopolysaccharides have complex and varied structures and knowledge of their chemical activity is crucial to the successful diagnosis of and vaccination against bacterial infections.

[1] To whom correspondence should be addressed at Laboratory of Biophysics, CBER/FDA HFM: 419, 1401 Rockville Pike, Rockville, MD, 20852-1448. Fax (301) 496-4684. E-mail: tebull@gandalf.cber.nih.gov.

The chemical activity of molecules in complex biological systems, such as those mentioned above, depends heavily on conformation. Conformational properties are especially important when considering very specific binding site interactions, and it is for this reason that disaccharide conformational studies are of interest.

Nuclear magnetic resonance (NMR) spectroscopy has proved to be an extremely powerful analytical tool for the structural and conformational analysis of monosaccharides, disaccharides, and polysaccharides in the past. NMR analyses can be especially helpful when combined with information from computer simulations of molecular dynamics (*1–4*). Experimental NMR data which have become invaluable in conformational investigations include homo- and heteronuclear as well as two-bond (*5–7*) and three-bond (*8, 9*) scalar coupling constants, nuclear Overhauser effects (NOEs) (*10, 11*), and spin–lattice and spin–spin relaxation rates (*12–14*). These experimental data can be measured as well as simulated, and the results provide information about the conformation of carbohydrate systems that may be difficult to obtain otherwise (*15, 16*).

NMR measurements of nuclear Overhauser enhancements are especially important in such conformational studies. NOEs are frequently measured using the NOESY experiment, a two-dimensional experiment allowing the determination of all observable NOEs within a system by making measurements at a number of mixing times (τ_m) in two time domains. However, when the NOE of interest is very small and many scans are required to obtain good signal to noise, the NOESY experiment requires very long experiment times.

A one-dimensional NOE measurement offers a solution to the problem. In such an experiment, collection of data points in the first time domain is eliminated, allowing a large number of additive scans to be acquired in the same amount of time and thus increasing the signal-to-noise ratio. The selectivity of NOE measurements can be enhanced by selectively exciting one nucleus in the molecule and observing only NOEs from nuclei that are coupled through space to that nucleus. This was the basis for the DPFGSE NOE (*17*) experiment as well as the GOESY (*18*) experiment, both shown in Fig. 1.

1090-7807/00 $35.00

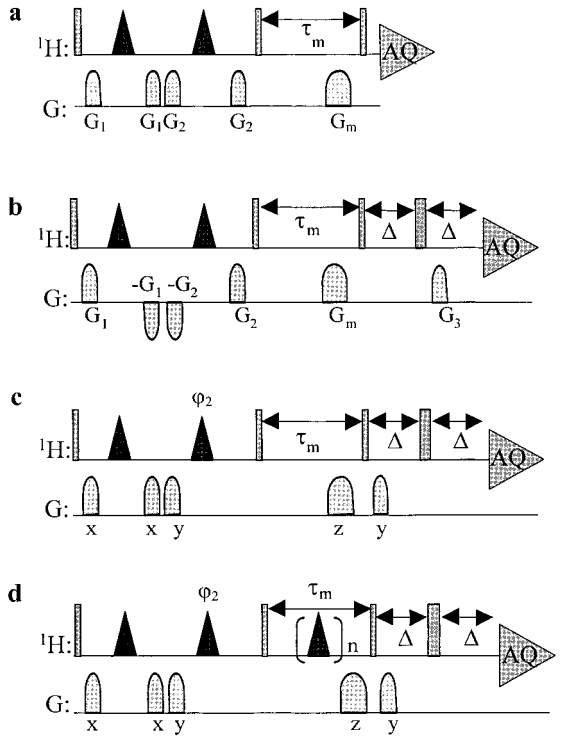

FIG. 1. The (a) DPFGSE NOE and (b) GOESY pulse sequences for selective measurement of 1D NOE spectra. The pulse sequence shown in (c) is the modified GOESY (M-GOESY) experiment developed here for the analysis of the α-L-Rha*p*-(1 → 2)-α-L-Rha*p*-OMe disaccharide. Addition of a selective inversion pulse during the mixing time, as shown in (d), reduces or eliminates indirect magnetization transfer during τ_m. Rectangles represent 90 and 180° hard proton pulses, and triangles represent 180° shaped pulses. All shaped pulses prior to τ_m are the i-SNOB-2 pulse form and are 50 ms in duration. The *x*, *y*, and *z* gradients in (c) and (d) were applied in a ratio of 1:1:2.5, respectively. All pulses were applied along the *x*-axis unless otherwise noted (φ_2 = 0, 1, 2, 3).

Peaks obtained using the DPFGSE NOE sequence contained contributions from spin–lattice relaxation to equilibrium during the mixing time, which were eliminated using difference spectroscopy. The GOESY sequence allowed the investigator to obtain the pure NOEs in one scan by phase encoding the target magnetization prior to the mixing time and decoding prior to acquisition. In the present study, a modified version of the GOESY pulse sequence (M-GOESY) was used to investigate the conformation of the disaccharide α-L-Rha*p*-(1 → 2)-α-L-Rha*p*-OMe, shown as **2** in Fig. 2.

Several studies of the conformations adopted by the disaccharide **2** have been carried out using both NMR and molecular dynamics simulations (*19–23*). Many of the simulations concluded that two stable conformations of the disaccharide were possible. The lowest energy conformers, termed A and B, have glycosidic torsion angles $\psi \approx 40°$ and $\psi \approx -30°$, respectively. In the Ramachandran map, a saddle point was observed in between the two conformers. Therefore, determination of the sign of the ψ torsion angle would allow the assignment of conformation.

2D NOESY NMR measurements were unable to provide conclusive evidence supporting a specific conformation due to the poor signal-to-noise ratios for the small NOEs of interest and the contribution of spin diffusion in one of the conformers. In the present study, 1D NOE techniques were applied to the conformational analysis of **2** in an attempt to more accurately measure long-range NOEs and thereby obtain more conclusive evidence of its conformational state(s).

EXPERIMENTAL

General

The monosaccharide, 1,6-anhydro-β-D-galactopyranoside (**1**), was obtained from the Department of Organic Chemistry, Stockholm University. The synthesis of the disaccharide α-L-Rha*p*-(1 → 2)-α-L-Rha*p*-OMe (**2**) and its analogue **2d**, deuterated at position 2 of the nonterminal sugar residue, has been described previously (*24*). The torsion angle ψ is described by C1′-O2-C2-H2, where a prime denotes atoms in the terminal sugar residue.

The monosaccharide **1** was dissolved in a 7:3 molar ratio of D_2O and dimethyl sulfoxide (DMSO-*d*6) to facilitate low-temperature experiments. A 50 mM solution of **1** was prepared from 100.0 atom% D D_2O (Aldrich, Wilwaukee) and 99.9 atom% D DMSO (Aldrich, Milwaukee, WI). Approximately 50 mM solutions of both **2** and **2d** were prepared in 100.0 atom% D D_2O. The samples were then placed in restricted-volume NMR tubes and sealed with matched susceptibility

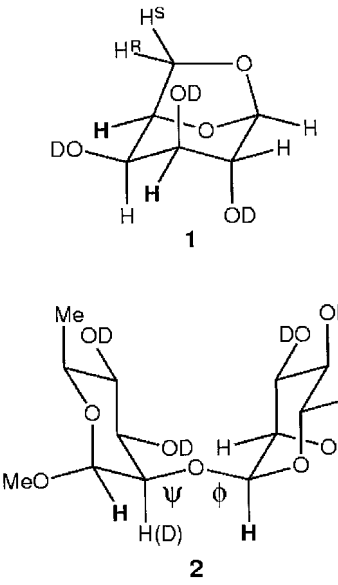

FIG. 2. Schematic of 1,6-anhydro-β-D-galactopyranoside (**1**) and α-L-Rha*p*-(1 → 2)-α-L-Rha*p*-OMe (**2**). The protons of interest are marked in bold, namely H3 and H5 in **1** and H1 and H1′ on either side of the glycosidic linkage in **2**. Glycosidic torsion angles are denoted by φ and ψ. In compound **2d**, the proton at C2 has been exchanged for a deuterium atom to alleviate possible indirect spin diffusion via H2.

plugs (Shigemi, Tokyo). No pH adjustments were performed on the resulting solutions and no attempt was made to remove dissolved oxygen from these samples.

Experimental Parameters

One-Dimensional NMR measurement of nuclear Overhauser enhancement. All NOE measurements were performed on a Bruker AM 500-MHz spectrometer equipped with a 5-mm *x*, *y*, *z*-gradient triple-resonance probe for PFG capability. Spectra of **1** were measured at a temperature of 243 K using a spectral width of 6024.1 Hz and 8192 data points. Spectra of **2** and **2d** were measured at a temperature of 310 K using a spectral width of 5050.50 Hz and 16384 data points. The total recycle time between scans was 7.8 s in the case of **2** and **2d** and 15.6 s in the case of **1**, approximately 4.5–6.0 times the longest T_1's. In all cases, the duration and power of the selective pulse were calibrated in order to yield 180° rotation of the target magnetization. Sinusoidal shaped *x*, *y*, and *z* gradients were applied in a ratio of 1:1:2.5, respectively. A set of 8 τ_m-values ranging from 0.025 to 0.200 s was used for the measurement of NOE buildup rates of the disaccharide, with 1–2K scans averaged at each τ_m-value. All measurements of the monosaccharide were performed with a constant mixing time of 600 ms and 256–512 scans. The FIDs were processed using FELIX 97.2 software on a Silicon Graphics Indigo 2 workstation. The FIDs were zero filled to 32K and multiplied with a decaying exponential, corresponding to 0.2–0.7 Hz of line broadening in the transformed spectrum, prior to Fourier transformation. Baseline correction was carried out by fitting selected baseline points to a first-order polynomial. In order to compensate for any drift in receiver amplification, apparent NOE buildup peak areas were divided by the area of the selectively excited peak to produce the normalized buildup intensity that was used to calculate NOE buildup rates (see Appendix).

Pulse Sequences

The pulse sequences used to measure the Overhauser magnetization transfer are shown in Fig. 1. Figure 1a shows the DPFGSE NOE sequence of Stott *et al.* (*17*) and, for the sake of comparison, Fig. 1b shows the GOESY pulse sequence as proposed by Stonehouse *et al.* (*18*). Figures 1c and 1d show the modified GOESY sequences used here, which combine aspects of both DPFGSE NOE and GOESY. In sequence 1c, the target proton is selectively excited using the "excitation sculpting" method of the DPFGSE NOE sequence, except that the magnetization is not decoded with a fourth pulsed field gradient before the mixing time. The target magnetization is then transferred to other protons during the mixing time, and a spoil gradient dephases any transverse magnetization at the end of the mixing time. Finally, the desired magnetization is decoded by a fifth gradient, and any chemical shift evolution is refocused.

In an attempt to suppress indirect transfer of magnetization through intermediate proton(s), sequence 1d incorporates the selective inversion of either (i) the intermediate proton suspected of indirect transfer or (ii) the source and target magnetization at the center of the mixing time. The second approach is similar to the 2D QUIET-NOESY experiment (*25, 26*) as well as the 1D experiment reported by Harris *et al.* (*27*) for the suppression of spin diffusion.

If the results differed between the experiments depicted in Figs. 1c and 1d, then the number of selective inversions during τ_m was increased and the results were extrapolated to an infinite number of inversions. In several of our trials using sequence 1d, two gradient pulses were applied during the mixing time, producing no change in the results obtained. In all sequences, the i-SNOB-2 pulse form (*28*) is used for selective π pulses.

The sequences in Figs. 1c and 1d are variations on the GOESY sequence (*18, 29*) that we will call M-GOESY for modified GOESY. M-GOESY is easier to set up than the original GOESY, since the first and second gradient pulses are identical, as are the third and fifth gradient pulses. In the original GOESY experiment, one or two pairs of gradient pulses of opposite polarity (and thus additive effects) encode the magnetization. Following the mixing time, the cumulative effect of all four encoding pulses is reversed in a final decoding pulse gradient. The M-GOESY sequence eliminates the need to tune the final decoding pulse gradient.

Since relaxation to equilibrium (RTE) during the mixing time is unidirectional, its contribution to the final signal is eliminated by the decoding gradient pulse following the mixing time. Comparison of NOE buildup peak heights resulting from DPFGSE NOE and M-GOESY analyses indicates that RTE contributes approximately 50% of the signal intensity in the DPFGSE NOE experiment, a finding consistent with previous reports (*29*).

RESULTS AND DISCUSSION

The intensity of the signal at nucleus j, I_j, following selective excitation of nucleus i in the pulse sequence in Fig. 1c is

$$I_j(\tau_m) = [-\sigma_{ij}\tau_m + O(\tau_m^2) - \cdots]I_i, \qquad [1]$$

where τ_m is the mixing time and σ_{ij} is the usual single spin to single spin Overhauser magnetization transfer rate (*30*). For a spherical molecule this rate is

$$\sigma_{ij} = \frac{3}{10}\frac{\gamma^4\hbar^2}{r_{ij}^6}\left[\frac{2\tau_c}{1+4\omega^2\tau_c^2} - \frac{\tau_c}{3}\right], \qquad [2]$$

where ω is the resonance frequency, γ is the magnetogyric

TABLE 1

NOE Buildup Rate σ_{53} of the Monosaccharide 1, and the Corresponding Distances r_{53}, as Obtained Using the M-GOESY Pulse Sequences in Figs. 1c and 1d

	M-GOESY pulse sequence		
	1c	1d (invert H4 during τ_m)	1d (invert H3/H5 during τ_m)
σ_{53} (exp.)	7.41×10^{-2} s^{-1}	1.72×10^{-2} s^{-1}	1.26×10^{-2} s^{-1}
r_{53} (exp.)	3.3 ± 0.17 Å	4.2 ± 0.21 Å	4.4 ± 0.20 Å
r_{53} (calc.)	4.3 Å	4.3 Å	4.3 Å

Note. Experimental r_{53} values are compared with r_{53} calculated from an energy minimized structure using CHARMM, in which $r_{12} = 2.5$ Å was used as a reference.

ratio, r_{ij} is the internuclear distance between nuclei i and j, and τ_c is the reorientational correlation time.

Dividing Eq. [1] by $\tau_m I_i$ gives

$$S_{ij} = I_j(\tau_m)/[\tau_m I_i] = -\sigma_{ij} \quad [3]$$

for sufficiently small τ_m. The ratio of two such quantities is

$$S_{ij}/S_{ik} = \sigma_{ij}/\sigma_{ik} \quad [4]$$

which, for a spherical molecule, reduces to

$$S_{ij}/S_{ik} = (r_{ik}/r_{ij})^6. \quad [5]$$

If the distance between nuclei i and j is constant and known, one can use the ratio of S_{ij} to S_{ik} to determine another internuclear distance, r_{ik}.

Equation [5] is usually correct for short internuclear distances. For larger distances, there is the possibility that magnetization may be transferred between two nuclei via a third, i.e., spin diffusion. And as shown by Widmalm *et al.* (*21*), this presents a problem in the analysis of the α-L-Rha*p*-(1 → 2)-α-L-Rha*p*-OMe disaccharide being considered here. Specifically, through a molecular dynamics simulation it was shown that the disaccharide could be in one of two conformations, termed A and B. Although the conformers are quite different, many of the internuclear distances are similar for the two. On the other hand, the distance between H1′ and H1 across the glycosidic bond ($r_{1'1}$) is quite different in the two forms. Nevertheless, they explained that the NOE transfer rates between H1′ and H1 are quite similar in the two forms as a result of indirect magnetization transfer via H2 in conformer B.

The effect of indirect magnetization transfer, or spin diffusion, has been studied in past investigations of both small molecules (*31, 32*) and macromolecules (*33, 34*). Indirect effects have been exploited in two basic ways in both one-dimensional and two-dimensional NMR experiments. They have been enhanced in order to gain additional structural information or information about a binding site (*35–38*), and they have also been reduced or eliminated in order to obtain accurate long-range internuclear distances (*27, 39–41*).

In order to distinguish between the two conformers of α-L-Rha*p*-(1 → 2)-α-L-Rha*p*-OMe in the present study, four sets of 1D NOE experiments were conducted using the M-GOESY sequence, three of which suppress the indirect transfer via an intermediate proton. In the active method of suppression, the indirect transfer of magnetization is inhibited by selective inversion of either the intermediate proton magnetization or the source and target proton magnetization in the middle of the mixing time. This selective inversion during the mixing time, suggested by Olejniczak *et al.* (*42*), can in theory be carried out a number of times in order to ensure complete cancellation. In practice, however, a previous report suggests that imperfect inversion of the magnetization as well as relaxation during the selective pulses limits the number of inversions which may be performed while still obtaining adequate sensitivity (*27*).

This methodology was validated on a simple model compound, namely the monosaccharide 1,6-anhydro-β-D-galactopyranoside (**1**). A representation of the structure of **1** is given in Fig. 2. The monosaccharide is a small and rigid molecule and for this reason was selected for study, as it would give rise to fairly strong indirect NOEs. To further ensure the likelihood of observing an indirect NOE, all experiments were performed

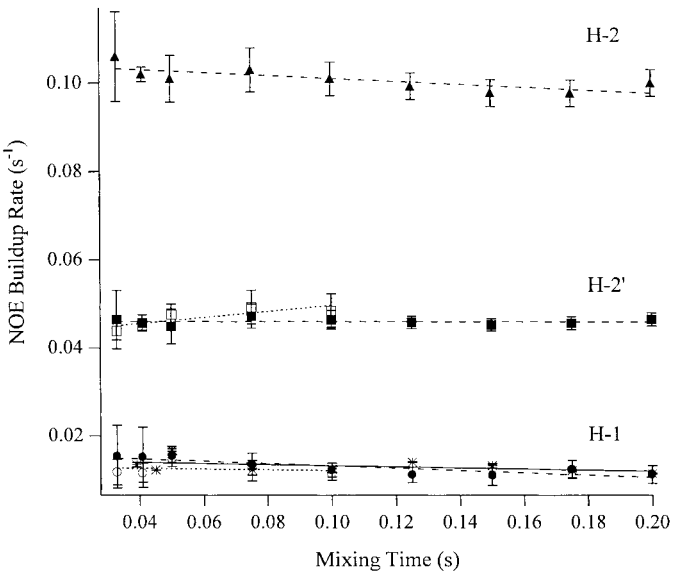

FIG. 3. Various plots of $I_j(\tau_m)/(\tau_m I_i)$ (i.e., the NOE buildup rate) versus τ_m for M-GOESY experiments applied to deuterated and nondeuterated α-L-Rha*p*-(1 → 2)-α-L-Rha*p*-OMe samples. The M-GOESY experiment without inversion during τ_m was used to obtain data for NOEs between H1′ and: (●) H1, (■) H2′, and (▲) H2 in the protonated sample as well as (○) H1 and (□) H2′ in the deuterated sample. The M-GOESY experiment with inversion of H2 during τ_m was used to measure NOEs between H1′ and H1 (✳) in the protonated sample only. Horizontal plots indicate that it is justified to neglect second- and higher-order terms in τ_m for the mixing times shown.

TABLE 2

Average NOE Buildup Rates $\sigma_{1'1}$, $\sigma_{1'2'}$, and $\sigma_{1'2}$ of 2 and 2d as Obtained Using the M-GOESY Pulse Sequences Shown in Fig. 1

M-GOESY pulse sequence	Compound	Average NOE buildup rate (σ_{ij}) ± standard deviation ($\times 10^2$ s^{-1})		$\sigma_{ij}/\sigma_{1'2'}$	r_{ij} (Å)
1c	**2**	$\sigma_{1'1}$	1.23 ± 0.18	0.27 ± 0.04	3.14
		$\sigma_{1'2'}$	4.60 ± 0.07		2.52[a]
		$\sigma_{1'2}$	10.1 ± 0.26	2.20 ± 0.27	2.21
1d (invert H2)	**2**	$\sigma_{1'1}$	1.31 ± 0.16	0.28 ± 0.03	3.11
1d (invert H1′/H1)	**2**	$\sigma_{1'1}$	1.26 ± 0.18	0.27 ± 0.04	3.13
1c (deuterate H2)	**2d**	$\sigma_{1'1}$	1.25 ± 0.14	0.27 ± 0.04	3.13
		$\sigma_{1'2'}$	4.57 ± 0.35		

Note. The final two columns show the appropriate ratios of σ's and the resulting internuclear distances.

[a] Reference internuclear distance obtained from Ref. (*21*).

at −30°C. The NOE between H5 and H3 was selected for study as it most probably contained an indirect component due to magnetization transfer through H4. The ^{1}H spectrum of **1** has been assigned previously (*43*). The 1D NOE spectra of **1** were acquired using the M-GOESY sequence as well as the M-GOESY sequence with one, three, and five selective inversions of H4 during the mixing time. The direct transfer rate was obtained by extrapolating the data acquired with one, three, and five inversions of H4 to an infinite number of inversions during τ_m. In this manner, two values for σ_{53} were obtained, one in the presence of indirect transfer through H4 and one in its absence, and these values are given in Table 1.

Also shown in Table 1 is the transfer rate σ_{53} obtained using the quiet M-GOESY, in which the source and target proton magnetization are inverted during the mixing time. The inversion was accomplished using a 100-ms phase modulated selective pulse, during which the transfer rate is a factor of 0.78 times slower than the normal NOE transfer rate. The final transfer rate was corrected to reflect this decreased transfer rate; however, the correction is not significant within the reported accuracy.

The two different methods of spin-diffusion suppression produce the same value, within error, for the internuclear distance r_{53}. Upon inversion of H4 during τ_m, an internuclear distance of 4.2 ± 0.21 Å is extracted, whereas inversion of H3 and H5 simultaneously yields a distance of 4.4 ± 0.20 Å. The value extracted from M-GOESY NMR data for r_{53} in the presence of indirect transfer is 3.3 ± 0.17 Å. Comparison of these data to the value for r_{53} of 4.3 Å, obtained from molecular mechanics calculations alone, indicates that the M-GOESY sequence shown in Fig. 1d effectively eliminates indirect NOE transfer and allows more accurate distance determination. This result also testifies to the inaccuracy of the long-range distances extracted from NOE data acquired using sequence 1c with a long mixing time.

Once the methodology was validated on the monosaccharide model, it was applied to the conformational analysis of the disaccharide. In experiment 1, H1′ was selectively excited and NOEs to H1 in the protonated sample were measured using the M-GOESY sequence shown in Fig. 1c. In experiment 2, any indirect transfer through proton H2 of conformer B was eliminated by deuteration of H2 and the experiments were repeated. In experiment 3, any indirect transfer via H2 was eliminated in the protonated sample by selective inversion of H2 in the middle of the mixing time using the M-GOESY sequence shown in Fig. 1d.

Figure 3 shows various plots of $I_j(\tau_m)/(\tau_m I_i)$ versus τ_m for the three experiments applied to both deuterated and nondeuterated α-L-Rha*p*-(1 → 2)-α-L-Rha*p*-OMe samples. The fact that these plots are nearly horizontal establishes that it is justified to neglect second- and higher-order terms in τ_m for the mixing times shown. In order to determine the values for the NOE buildup rates, σ_{ij}, one could in theory extrapolate these plots to $\tau_m = 0$. We have chosen, however, to use the average of the values of σ_{ij} calculated at the various mixing times shown (see Appendix). Table 2 summarizes the data and the resulting internuclear distances calculated according to Eq. [5].

Table 2 also contains the results from the quiet version of M-GOESY in which H1′ and H1 are both inverted during the

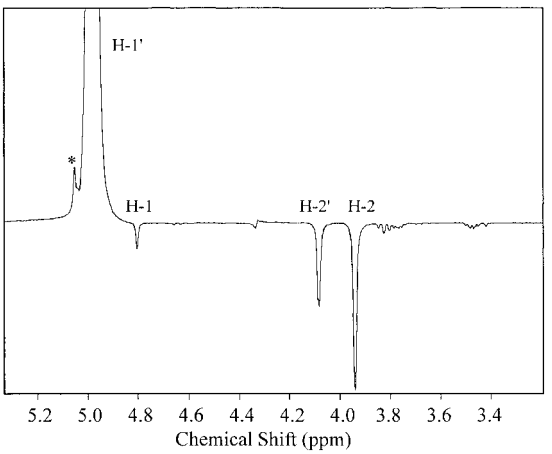

FIG. 4. 1D M-GOESY NOE spectrum of **2**, with arbitrary phasing of source and NOE buildup peaks. As shown, the NOE of interest between H1′ and H1 is small. The asterisk (*) marks an impurity in the sample.

TABLE 3

Comparison of Results from M-GOESY Analysis to Those Obtained by Molecular Mechanics Simulation for the Disaccharide 2

	Internuclear distances (Å)		
	M-GOESY: experimental	Simulation: conformation A	Simulation: conformation B
$r_{1'1}$	3.1	3.24	4.43
$r_{1'2}$	2.2	2.32	2.58

mixing time. Due to the proximity of the H1′ and H1 resonances in the spectrum of **2**, the inversion was accomplished using a single 17.5-ms, unmodulated selective pulse during which the transfer rate is a factor of approximately 1.02 times greater than the normal NOE transfer rate. The reported transfer rate was again corrected to reflect this increased transfer rate. However, as before, the correction is not significant within the reported accuracy.

As shown in Fig. 4, the NOE of interest between H1 and H1′ is quite small and measurement of such an NOE results in approximately 10–15% error at short mixing times. Regardless, the magnetization transfer rate between H1′ and H1 is the same, within error, for all the experiments performed. This result indicates that indirect magnetization transfer, either via H2 or other neighboring protons, does not make a significant contribution to the apparent transfer rate $\sigma_{1'1}$. Consequently, the α-L-Rha*p*-(1 $\rightarrow$ 2)-α-L-Rha*p*-OMe disaccharide must be predominantly in conformation A where the torsion angle ψ is negative and the indirect transfer via H2 is negligible (*21*). The same conclusion is reached when internuclear distances calculated from the M-GOESY experiment are compared with the results of the molecular mechanics simulations (*19*), as shown in Table 3. The previously determined *trans*-glycosidic $^3J_{C,H}$ values (*20*) indicate, via a Karplus-type relationship, that the magnitude of the ψ torsion angle should be slightly lower than in the pure A conformer. The combined evidence from NOEs in this study, past $^3J_{C,H}$ values, and molecular mechanics/molecular dynamics simulations show a single major conformer with the glycosidic torsion angle $\psi \approx -30°$.

CONCLUSIONS

Like GOESY, the M-GOESY method allows investigations of very small NOEs to a specific nucleus. M-GOESY produces pure NOEs that contain no contribution from relaxation to equilibrium in a single scan by gradient encoding and decoding the magnetization before and after the mixing time. In this way, the need for acquisition and subtraction of reference spectra is eliminated. Unlike GOESY, however, M-GOESY does not require any tuning of gradient pulses.

The M-GOESY experiment, with and without elimination of indirect magnetization transfer, was validated using the monosaccharide 1,6-anhydro-β-D-galactopyranoside. M-GOESY with selective inversion(s) during the mixing time was found to effectively eliminate any indirect contributions to the observed NOE buildup rate, allowing more accurate calculation of long-range internuclear distances. The experiment was then applied to the conformational analysis of the disaccharide α-L-Rha*p*-(1 $\rightarrow$ 2)-α-L-Rha*p*-OMe. Two possible conformations of the disaccharide were proposed using molecular dynamics simulations and NOE data, and of those two the M-GOESY analysis indicates that the molecule exists predominantly in conformation A with a negative ψ torsion angle.

APPENDIX

The master equation for NOE magnetization transfer and relaxation is

$$dI(t)/dt = -RI(t), \qquad [A1]$$

where R is the relaxation matrix and $I(t)$ is the vector of nuclear spin magnetizations. Equation [A1] has the formal solution

$$I(t) = \exp(-Rt)I(0). \qquad [A2]$$

At short times and with the initial condition $I(0) = I_i(0)$, this becomes

$$I_j(t) = -\sigma_{ij}tI_i(0) \qquad [A3]$$

or

$$I_j(t)/[tI_i(0)] = -\sigma_{ij} \qquad [A4]$$

to zeroth order in t.

A more precise approximation can be derived as follows. With the same initial condition and at short times, one can rewrite Eq. [A1] as

$$dI_j(t)/dt = \Delta I_j(t)/\Delta t = I_j(t)/t = -\sigma_{ij}I_i(t) \qquad [A5]$$

or

$$I_j(t)/[tI_i(t)] = -\sigma_{ij}. \qquad [A6]$$

It can be shown that with the specified initial conditions Eqs. [A6] and [A4] are related by the expression

$$I_j(t)/[tI_i(t)] = I_j(t)/[tI_i(0)] - \sigma_{ij}\rho_i t \qquad [A7]$$

to first order in t, where ρ_i is the auto relaxation rate of I_i. For a two-spin system the first-order correction to Eq. [A4]

is $+ \sigma_{ij}(\rho_i + \rho_j)t/2$. Consequently, if $\rho_i = \rho_j$, Eq. [A6] is correct to first order in t, whereas Eq. [A4] is valid only to zeroth order in t. For a system with a larger number of spins or one where the auto relaxation rates are not equal, the cancellation of terms to first order in t is not exact, but use of Eq. [A6] will greatly reduce the higher-order corrections to the approximation.

A further advantage of using Eq. [A6] is that the calculated value is independent of the spectrometer's receiver gain, since it involves the ratio of two magnetizations within the same spectrum rather than a ratio of magnetizations from different spectra.

Inspection of Fig. 4 shows that approximations leading to Eq. [A6] are valid for all of the mixing times reported. Therefore, the experimental data reported in this article are derived from the calculated value of the expression on the left-hand side of Eq. [A6] averaged over the various mixing times.

ACKNOWLEDGMENTS

The authors acknowledge the Molecular Modeling Interest Group at the National Institutes of Health for access to Felix 97.2 software. A.M.D. thanks Dr. D. Freedberg for helpful discussions. This research was supported in part by an appointment to the Postgraduate Research Program at the Centers for Biologics Evaluation and Research administered by the Oak Ridge Institute for Science and Education through an interagency agreement between the U.S. Department of Energy and the U.S. Food and Drug Administration. This work was also supported in part by a grant from the Swedish Natural Science Research Council.

REFERENCES

1. C. Landersjö, R. Stenutz, and G. Widmalm, *J. Am. Chem. Soc.* **119,** 8695–8698 (1997).
2. I. Braccini, R. P. Grasso, and S. Pérez, *Carbohydr. Res.* **317,** 119–130 (1999).
3. C. A. Stortz, *Carbohydr. Res.* **322,** 77–86 (1999).
4. A. Vishnyakov, G. Widmalm, J. Kowalewski, and A. Laaksonen, *J. Am. Chem. Soc.* **121,** 5403–5412 (1999).
5. H. G. Bazin, I. Capila, and R. J. Linhardt, *Carbohydr. Res.* **309,** 135–144 (1998).
6. S. Zhao, G. Bondo, J. Zajicek, and A. S. Serianni, *Carbohydr. Res.* **309,** 145–152 (1998).
7. G. Batta and K. E. Kövér, *Carbohydr. Res.* **320,** 267–272 (1999).
8. B. Bose, S. Zhao, R. Stenutz, F. Cloran, P. B. Bondo, G. Bond, B. Hertz, I. Carmichael, and A. S. Serianni, *J. Am. Chem. Soc.* **120,** 11158–11173 (1998).
9. F. Cloran, I. Carmichael, and A. S. Serianni, *J. Am. Chem. Soc.* **121,** 9843–9851 (1999).
10. N. Bouchemal-Chibani, I. Braccini, C. Derouet, C. Hervé du Penhoat, and V. Michon, *Int. J. Biol. Macromol.* **17,** 177–182 (1995).
11. U. R. Desai, I. R. Vlahov, A. Pervin, and R. J. Linhardt, *Carbohydr. Res.* **275,** 391–401 (1995).
12. D. C. McCain and J. L. Markley, *Carbohydr. Res.* **152,** 73–80 (1986).
13. L. Mäler, G. Widmalm, and J. Kowalewski, *J. Phys. Chem.* **100,** 17103–17110 (1996).
14. A. Geyer, M. Müller, and R. R. Schmidt, *J. Am. Chem. Soc.* **121,** 6312–6313 (1999).
15. C. Hervé du Penhoat, A. Imberty, N. Roques, V. Michon, J. Mentech, G. Descotes, and S. Pérez, *J. Am. Chem. Soc.* **113,** 3720–3727 (1991).
16. G. Batta, K. E. Kövér, J. Gervay, M. Hornyák, and G. M. Roberts, *J. Am. Chem. Soc.* **119,** 1336–1345 (1997).
17. K. Stott, J. Stonehouse, T. L. Hwang, J. Keeler, and A. J. Shaka, *J. Am. Chem. Soc.* **117,** 4199–4200 (1995).
18. J. Stonehouse, P. Adell, J. Keeler, and A. J. Shaka, *J. Am. Chem. Soc.* **116,** 6037–6038 (1994).
19. B. J. Hardy, W. Egan, and G. Widmalm, *Int. J. Biol. Marcromol.* **17,** 149–160 (1995).
20. B. J. Hardy, S. Bystricky, P. Kovac, and G. Widmalm, *Biopolymers* **41,** 83–96 (1997).
21. G. Widmalm, R. A Byrd, and W. Egan, *Carbohydr. Res.* **229,** 195–211 (1992).
22. T. Kozár, N. E. Nifant'ev, H. Grosskurth, U. Dabrowski, and J. Dabrowski, *Biopolymers* **46,** 417–432 (1998).
23. P. Jansson, L. Kenne, and G. Widmalm, *Acta Chem. Scand.* **45,** 517–522 (1991).
24. P. Söderman, S. Oscarson, and G. Widmalm, *Carbohydr. Res.* **312,** 233–237 (1998).
25. C. Zwahlen, S. J. F. Vincent, L. Di Bari, M. H. Levitt, and G. Bodenhausen, *J. Am. Chem. Soc.* **116,** 362–368 (1994).
26. S. J. F. Vincent, C. Zwahlen, and G. Bodenhausen, *J. Biomol. NMR* **7,** 169–172 (1996).
27. G. J. Harris, N. Patel, B. J. Rawlings, and T. J. Norwood, *J. Magn. Reson.* **140,** 504–509 (1999).
28. Ē. Kupče, J. Boyd, and I. D. Campbell, *J. Magn. Reson. B* **106,** 300–303 (1995).
29. K. Stott, J. Keeler, Q. N. Van, and A. J. Shaka, *J. Magn. Reson.* **125,** 302–324 (1997).
30. T. E. Bull, *Prog. NMR Spectrosc.* **24,** 377–410 (1992).
31. G. Batta, K. E. Kövér, and Z. Mádi, *J. Magn. Reson.* **73,** 477–486 (1987).
32. J. Redondo, F. Sánchez-Ferrando, M. Valls, and A. Virgili, *Magn. Reson. Chem.* **26,** 511–517 (1988).
33. A. N. Lane, *J. Magn. Reson.* **78,** 425–439 (1988).
34. V. V. Krishnan, U. Hegde, and A. Kumar, *J. Magn. Reson.* **94,** 605–611 (1991).
35. K. E. Kövér and G. Batta, *J. Am. Chem. Soc.* **107,** 5829–5830 (1985).
36. K. E. Kövér and G. Batta, *Magn. Reson. Chem.* **26,** 181–184 (1988).
37. R. Boelens, G. W. Vuister, T. M. G. Koning, and R. Kaptein, *J. Am. Chem. Soc.* **111,** 8525–8526 (1989).
38. S. R. Arepalli, C. P. J. Glaudemans, G. D. Daves, Jr., P. Kovac, and A. Bax, *J. Magn. Reson. B* **106,** 195–198 (1995).
39. W. Massefski, Jr., and A. G. Redfield, *J. Magn. Reson.* **78,** 150–155 (1988).
40. J. Fejzo, A. M. Krezel, W. M. Westler, S. Macura, and J. L. Markley, *J. Magn. Reson.* **92,** 651–657 (1991).
41. C. G. Hoogstraten, W. M. Westler, S. Macura, and J. L. Markley, *J. Am. Chem. Soc.* **117,** 5610–5611 (1995).
42. E. T. Olejniczak, R. T. Gampe, Jr., and S. W. Fesik, *J. Magn. Reson.* **67,** 28–41 (1986).
43. T. Nishida, G. Widmalm, and P. Sandor, *Magn. Reson. Chem.* **34,** 377–382 (1996).